SAWater
stewardship council trust

University of Strathclyde Engineering

Acid Mine Drainage in the Western Pits, South Africa - a box model for biotic Pyrite Oxidation

CL973 Independent Study in Collaboration with Industry

UNIVERSITY OF STRATHCLYDE

DEPARTMENT OF CIVIL AND ENVIRONMENTAL ENGINEERING

March 28, 2014

Authored by: **Lisa Wild, MSc Hydrogeology**
Registration Number: 201385395

ABSTRACT

Acid mine drainage is a major problem in abandoned mines all over the world. The Western Pits near Johannesburg, South Africa are one of those abandoned mine shafts. Acid mine drainage has been observed and investigations are running to elaborate the scope and a remediation options. This report aims to support these investigations and analyse underground pyrite oxidation pathways of the acid mine drainage conceptual model designed by Anthony Turton, Water Stewardship Council of Southern Africa.

First a detailed conceptual box model of the underground pathway was designed to derive a better understanding of the problem. As a result, an excel spread sheet was designed to calculate the increasing concentration of H^+ that was produced by underground pyrite oxidation in the presence of the bacterium *Acidithiobacillus ferrooxidans*. By analysing the concentration of H^+, first the mass load of sulphuric acid was calculated and consequently the pH to examine the influence of pyrite oxidation on acidity.

In order to find an appropriate remediation option for acid mine drainage, the box model was extended by introducing the buffer capacity of calcium carbonate for sulphuric acid.

The results showed that the H^+ concentration increased over time when meanwhile the pH was decreasing. As a result the mass load of sulphuric acid rose as well. Due to the rising mass load of sulphuric acid, the required amount of calcium carbonate per day to buffer the acidity was also increasing.

In conclusion the Excel Box model gave good and reasonable results, even though the input data was mostly assumed or from literature. To elaborate the box model, further data should be collected during field work and laboratory experiments.

TABLE OF CONTENTS

1. INTRODUCTION 1
2. Aims and Objectives 2
3. Theoretical Principles 3
4. Methodology 4
4.1. Conceptual Box Model for pathway D 4
4.2. Evolving an Excel Spreadsheet 5
4.2.1. Calculating the generated H^+ Concentration 5
4.2.2. Mass flow of sulphuric acid 7
4.2.3. pH-change over time 7
4.3. Buffer Capacity of calcium carbonate 7
5. Results and Discussion 9
5.1. Rate of acid produced per day 9
5.2. Change in H^+ concentration over time 9
5.3. Mass flow of sulphuric acid 10
5.4. pH - change over time 10
5.5. Mass flow of calcium carbonate 11
5.6. The Influence of Pyrite oxidation on Heavy Metals and Uranium 12
6. Conclusion and Recommendations 13
7. References 14

1. INTRODUCTION

The city of Johannesburg has only become what it is today because of gold mining. In 1886 a gold reef was found accidentally and shortly after, a massive gold rush and thousands of new settlers have arrived. 30 years later the largest city of South Africa was born (City of Johannesburg, 2014). Now, almost 130 years later, the mining history brings disgrace on Johannesburg's region; Acid Mine Drainage (AMD) has become one of the biggest problems worldwide. In South Africa the media describe AMD as the poisonous waters that rise "inexorably" towards the city of Johannesburg and as a "ticking time bomb" (York, 2010).

But what really is acid mine drainage? It can be described as the drainage that results from the oxidation of pyrite or other sulphide minerals when mine rock co-occurs with water and oxygen (Bell, 1998). During the mining process groundwater is pumped to drop the water table. However after a mine is exploited and the mining company abandons the shaft, pumping stops and water can ingress into the mine voids and from this point onwards pyrite oxidation can take place. Acid mine drainage decants in the lowest shafts and is then mostly point discharged from the underground mines. It is known to be very acidic and to contain high concentrations of metals (Fe, Al, Mn, toxic heavy metals) and metalloids (mainly arsenic) (Johnson and Hallberg, 2005). To prevent further ecological disasters like extensive water contamination and fish dying, four pathways (shown in Figure 1) have been investigated by Anthony Turton to develop remediation options.

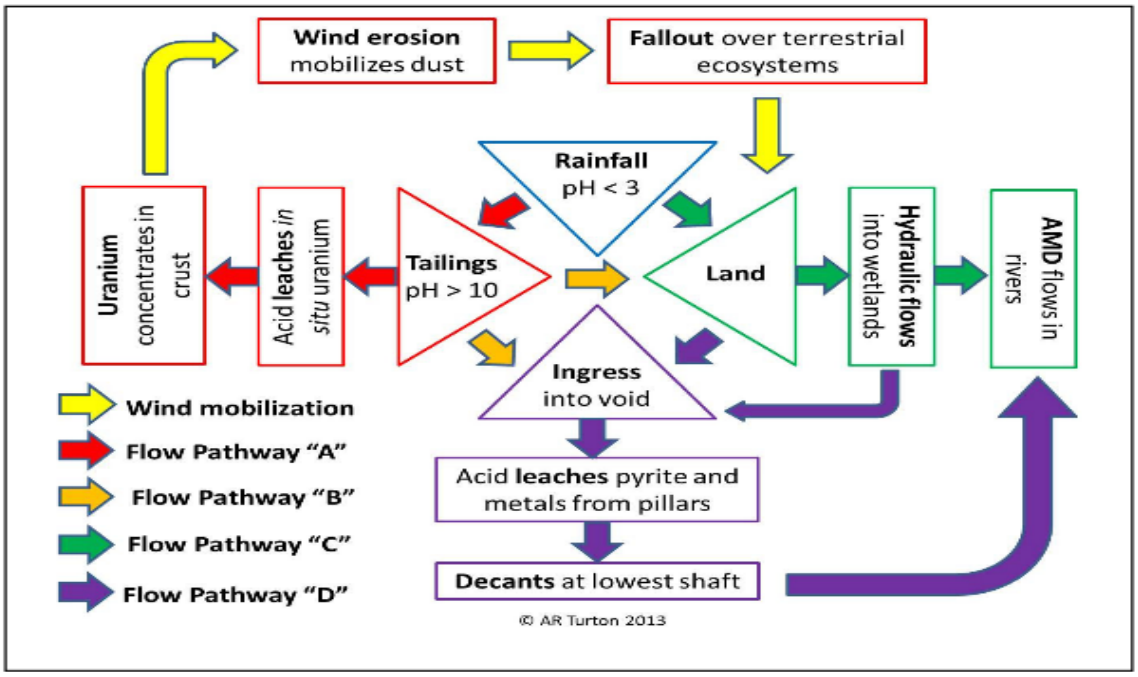

Figure 1 displays the four pathways of acid mine drainage (Turton, 2013)

Pathway A is the acid rain infiltration on mine dumps. The initial pH was determined to be 10 and overtime the dumps acidify. The main problem here is the uranium mobilisation. At a pH of lower than 5 or higher than 10, soluble uranium compounds can be generated (Casas et al., 1998).

Pathway B consists of the tailing dump runoff to either the wetlands (Pathway C), where a kind of bioremediation of the acid mine drainage takes place or to the underground voids (Pathway D). The Pathway D describes the pyrite oxidation that takes place underground.

The study concentrates on the Randfontain and Krugersdorp area (outskirts of Johannesburg) where gold mining industry has created large underground mine voids. Water that has decanted in the lowest shafts, has been detected to rise and acid mine drainage has been observed in form of “yellow boy” and acidic waters. In the following, pathway D will be examined thoroughly to create a conceptual box model resulting in an Excel box model which estimates the pH over time and the capacity of Calcium carbonate ($CaCO_3$) to buffer the acidic solution.

2. AIMS AND OBJECTIVES

1) Understand the principles of pyrite oxidation and acid mine drainage
2) Design a box model in excel to assess the rate of sulphuric acid production
3) Evaluate the impact of the pH behaviour
4) Assess the buffer capacity of calcium carbonate and calculate the required mass flow with the Excel spread sheet

The general aim is therefore the design of a model that offers the opportunity to understand the extent of pyrite oxidation in the underground mines.

3. THEORETICAL PRINCIPLES

The main process that takes place in the underground mine shafts is the oxidation of Pyrite (FeS_2). Pyrite is also known as “fool’s gold” and one of the most common sulphide minerals in sedimentary rock, but occurs also in igneous and metamorphic rocks in small proportions (Hawkins, 2014).

Biotic pyrite oxidation takes place in presence of the bacterium *Acidithiobacillus ferrooxidans*. *A.ferrooxidans* was first isolated by Colmer and Hinkle in 1947 from acid mine drainage of a coal mine in West Virginia, United States of America. At this point the problem of acid mine drainage was already prevalent and a solution to the problem was sought. With this finding, the assumption was taken that the availability of air is not the only criterion for the process of pyrite oxidation (Colmer et al., 1947).

Further research identified that the bacterium enhances the reaction rate with a factor of more than 10^6 in relation to the abiotic environment (Gleisner et al., 2006). This can be explained by the chemolithoautotrophic metabolism of the microorganism, that indicates the oxidation of sulphide compounds as well as bivalent iron (Fe^{2+}), which can be used as an electron-donor. Therefore *A.ferrooxidans* does not necessarily need oxygen to oxidise pyrite (Leduc and Ferroni, 1994). However the reaction rate accelerates with increasing dissolved oxygen concentration (Gleisner et al., 2006).
The microorganism *A. ferrooxidans* is most active in acidic waters with a pH around 3.2, which means the conditions need to be acidic in the first place so that *A.ferrooxidans* can work effectively and further acidity is generated (Bell, 1998).

The chemical reaction for pyrite oxidation starts with the oxidation of pyrite to release ferrous iron (Fe^{2+}) (Equation 1).

$$FeS_2 + 3.5O_2 + H_2O \rightarrow Fe^{2+} + 2SO_4^{2-} + 2H^+ \quad (1)$$

Ferrous iron is then oxidised by *A.ferrooxidans* to ferric iron (Fe^{3+}) (Equation 2).

$$2Fe^{2+} + 0.5O_2 + 2H^+ \rightarrow 2Fe^{3+} + H_2O \quad (2)$$

Ferric iron is then used as an electron acceptor instead of oxygen to oxidise pyrite and water so that more ferrous iron, H^+ and sulphate is released (Equation 3)

$$FeS_2 + 14Fe^{3+} + 8H_2O \rightarrow 15Fe^{2+} + 2SO_4^{2-} + 16H^+ \quad (3)$$

In the acid mine drainage (pH<4.5) ferrous iron is again oxidised to ferric iron by *A.ferroxidans*, which creates a cyclic process. When the pH of the acid mine drainage outflow increases to over 4.5, after reaching a river for instance, iron hydroxide (“yellow boy”) is precipitated (Equation 4).

$$4Fe^{3+} + 12H_2O \rightarrow 4Fe(OH)_3 + 12H^+ \quad (4)$$

4. METHODOLOGY

4.1. CONCEPTUAL BOX MODEL FOR PATHWAY D

To get a better understanding of the problem and the in- and outflows of the system, a box model was created from the drafts of Tony Turton's overall box model (Turton, 2013). The model in Figure 2 conceptualises the flows and reaction mechanisms of the pyrite oxidation implemented by the sulphide consuming bacteria *Acidithiobacillus ferrooxidans*.

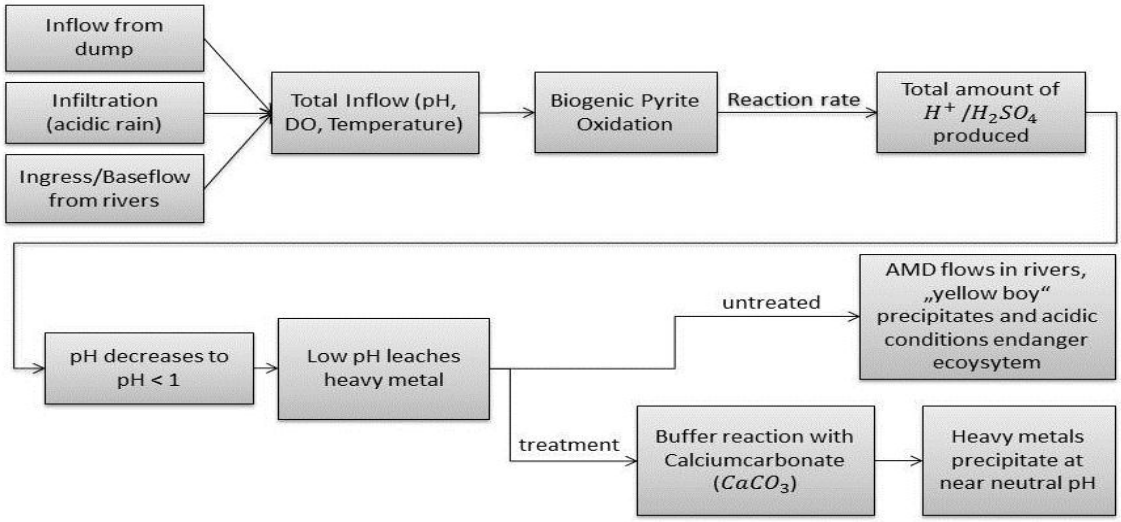

Figure 2 shows the conceptual model of pyrite oxidation in mine pillars underground

In this first understanding, inflows to the remaining pillars, which are the protection areas that have been kept untouched during mining process to provide mines from collapsing, come from different sources. Three inflows can be discussed and measured to become the total flow: the runoff-water that ingresses the voids through the entrances of the mineshafts, the infiltration of rainfall, which can also be described as acid rain and the baseflow from rivers to the groundwater of the mineshafts. With a reaction rate and the volume of the inflow, the amount of produced sulphuric acid (H_2SO_4) due to biogenic pyrite oxidation can be calculated. The produced sulphuric acid exacerbates the acidity in the already acidic environment and therefore leaches heavy metals that are only soluble in very acidic environment. Without treatment the AMD, which now consists of mobilized heavy metals in a very acidic solution potentially flows into rivers and surface waters. The mixing process with neutral waters increase the pH to a pH < 4.5 where iron hydroxide ("yellow boy") precipitates, as shown in Figure 3.

Figure 3 shows yellow boy in a river downstream of the Wester pits (left side) and coal mine in the Brugspruit Valley (right side), (Turton, 2013) and (Greenpeace, 2011)

Elaborating a treatment process for the acid mine drainage, the outflow could be redirected to a reaction pond containing calcium carbonate or limestone. In this process the acid mine drainage would be neutralized. A more detailed description is given in chapter 4.3.

4.2. EVOLVING AN EXCEL SPREADSHEET

After understanding the principles of the processes taking place in the mine shafts,the calculation of how much more acidic the water will become with the influence of *A.ferrooooxidans* is now described.

4.2.1. CALCULATING THE GENERATED H^+ CONCENTRATION

Equation 5, which was derived from Gleisner et al., (2006), is the basis to calculate the subsequent concentration of H^+ in solution.

$$c_i = R_{FeS_2-i} * A_{BET} * m * x_i \qquad \text{[mol/L]} \qquad (5)$$

Where:

c_i = the concentration of H^+ after reaction has taken place

R_{FeS_2-i} = the biotic reaction rate for pyrite oxidation [mol/(m^2 s)]

A_{BET} = the specific surface of the pyrite grains [m^2/g]

m = the mass of pyrite grains [g]

x_i = stoichiometric factor (1 for Fe and 2 for S) [-]

Establishing these parameters turned out to be quite challenging as the specific surface area as well as the reaction rate should be tested in laboratory analyses. When the runoff tailings pond of IL 8 was sampled, following parameters were obtained:

pH = **2.68** Temperature = 23.8°C

DO (dissolved oxygen) = 6.52 mg/L

$$= \frac{6.52\ \text{mg}}{\text{l}*1000\ \text{ml}} * \frac{1\ \text{mol}*1000\ \text{mmol}}{31.9988\ \text{g}*1000\ \text{mg}} = 0.00020376\ \text{mM} = \mathbf{0.2037\mu M}$$

Gleisner et al.(2006) calculated various pyrite oxidation rates for pH 3 at different dissolved oxygen concentrations from their experiments. Table 1 shows the pyrite oxidation rates for 273, 129, 64.8, 13.2 and ≤ 0.006 µM. As the dissolved oxygen concentration for the Western Pits was measured with 0.2037µM and none of the experiments was conducted with exactly this concentration only an approximate reaction rate can be assumed.

Table 1 Pyrite oxidation rates at various DO levels (Gleisner et al., 2006)

Concentration of planktonic bacteria and pyrite oxidation rates, R_{FeS_2-S} and R_{FeS_2-Fe}, in pyrite oxidation experiments by *A. ferrooxidans* at various DO levels

DO concentration, µM	Bacterial concentration		Pyrite oxidation rate	
	Day 51 (cells/mL) × 10^6	Day 64 (cells/mL) × 10^6	R_{FeS_2-S} (mol m^{-2} s^{-1} × 10^{-10})	R_{FeS_2-Fe} (mol m^{-2} s^{-1} × 10^{-10})
273	11.4, 25.8	21.30, 27.41	5.01, 8.91	4.51, 7.71
129	3.48, 1.35	4.01, 1.91	4.06, 2.14	3.54, 1.27
64.8	4.13, 1.36	4.02, 6.83	2.22, 2.91	1.11, 2.02
13.2[a]	1.30	1.86	0.192	0.0254
≤0.006	0.34, 1.52	0.41, 1.97	0.0192, 0.178	0.0072, 0.0196

Values separated by commas indicate results for duplicate experiments.
[a] Only single reactor at [DO]=13.2 µM.

As the DO concentration of the Western pits is closest to 13.2 µM the reaction rate for sulphide was used for further calculations:

$$\mathrm{R_{FeS_2-S}} = \mathbf{0.192 * 10^{-10}}\ \frac{\text{mol}}{m^2 * s}$$

The specific surface area can either be determined with laboratory tests using N_2 adsorption and Brunnauer-Emmett-Teller (BET) (Gleisner et al., 2006) or calculated with different parameters (Lapakko and Antonson, 2006), but as no information was available, a value from literature was adopted:

$$\mathrm{A_{BET}} = 0.147\ \mathrm{m^2/g}$$

In reality this value might be smaller, as the pyrite, used for this analysis, was crushed to very small grain sizes (63 µm and 250 µm) (Gleisner et al., 2006).

The total mass of pyrite grains was assumed to be 50 tonnes and the stoichiometric factor was 2. By taking the produced moles per day and

dividing it by the total inflow of the system (50 ML/day), the concentration change per day can be calculated.

4.2.2. MASS FLOW OF SULPHURIC ACID

As the molar concentration (mol/L) was already calculated, it only needs to be transformed into a mass concentration (g/L) for sulphuric acid by using Equation 6 and the molar mass M of sulphuric acid (98.079 g/mol).

$$n = \frac{m}{M} = \frac{\text{mass [g]}}{\text{Molar mass [g mol}^{-1}\text{]}} \rightarrow m = n * M \text{ [g]} \quad (6)$$

The mass concentration (g/L) is then transformed into a mass flow (kg/d) multiplying with the volumetric flow (L/d).

$$\dot{m} = \dot{v} * c \text{ [kg/d]} \quad (7)$$

4.2.3. PH-CHANGE OVER TIME

Knowing the concentration of H^+ generated by the pyrite oxidation by *A.ferrooxidans* and the initial pH, the final pH can be calculated.

First the initial pH 2.68 is transformed into the concentration of H^+ in solution with Equation 8. Then this initial concentration is added to the concentration change and finally the total concentration can be calculated back to pH by using equation 9. The results where then plotted in a diagram over time shown in the results section.

$$pH = -\log [H^+] \quad (8)$$

$$[H^+] = 10^{-pH} \quad (9)$$

4.3. BUFFER CAPACITY OF CALCIUM CARBONATE

Generally regions with limestone bedrock usually have no problems with acid rain weathering. The reason for this is that limestone is composed mainly of calcium carbonate ($CaCO_3$) and rock that contains sufficient amounts of $CaCO_3$ creates an excellent buffer system (Krug and Frink, 1983). This buffering capacity can hold the pH constant when small quantity of acid or base are added to the solution.

In the groundwater system of the Western Pits, the conditions do not imply the presence of calcite in the rock and therefore no natural buffer system exists. The idea now is to add calcium carbonate to evolve an artificial buffer solution, so that the produced sulphuric acid from *A.ferrooxidans* cannot exert any negative effects as it is neutralised by the calcium carbonate.

The chemical reaction can be explained as follows. The solution consists of sulphuric acid (H_2SO_4) dissociating to bisulphate (HSO_4^-) and Hydronium (H_3O^+) (Equation 12) and the added calcium carbonate ($CaCO_3$), dissolving to a greater or lesser extent to calcium (Ca^{2+}) and carbonate (CO_3^{2-}) (Equation 13).

Equation 12 shows that calcium (Ca^{2+}) precipitates then with bisulphate (HSO_4^-) to calcium sulphate ($CaSO_4$) and releases a proton (H^+). Two H^+ react with carbonate (CO_3^-) to carbonic acid (H_2CO_3), which is however unstable in water and therefore decomposes either into bicarbonate (HCO_3^-) and H^+ (Equation 13) or dissociates further to carbon dioxide (CO_2) and water (H_2O) (Equation 14) (Bishop, 2002).

$$H_2SO_4 + H_2O \rightleftharpoons H_3O^+ + HSO_4^- \quad (10)$$

$$CaCO_3 \rightleftharpoons Ca^{2+} + CO_3^{2-} \quad (11)$$

$$HSO_4^- + Ca^{2+} \rightleftharpoons CaSO_4 \downarrow + H^+ \quad (12)$$

$$2H^+ + CO_3^- \rightleftharpoons H_2CO_3 \rightleftharpoons H^+ + HCO_3^- \quad (13)$$

$$H^+ + HCO_3^- \rightleftharpoons H_2CO_3 \rightleftharpoons CO_2 + H_2O \quad (14)$$

Depending on the pH of the solution the following reactions are possible:

$$2CaCO_{3(s)} + 2H^+ + SO_4^{2-} \rightleftharpoons 2Ca^{2+} + SO_4^{2-} + 2HCO_3^- \quad (15)$$

$$CaCO_{3(s)} + H_2SO_{4(aq)} \rightleftharpoons CaSO_{4(aq)} \downarrow + CO_{2(g)} \uparrow + H_2O_{(aq)} \quad (16)$$

As the groundwater in the Western Pits is very acidic and sulphuric acid is a strong acid, Equation 16 will only take place when an excess amount of calcium carbonate is added. In that case calcium sulphate ($CaSO_4$), carbon dioxide (CO_2) and water (H_2O) are being produced and the water is neutralised.

The desired overall equation is shown in Equation 16. According to this, 1 mole of calcium carbonate neutralizes 1 mole of sulphuric acid (H_2SO_4).

$$n\,(CaCO_3) = n\,(H_2SO_4) = 1 \quad (15)$$

By knowing the concentration of H+ and the volume flow, the required mass of calcium carbonate ($CaCO_3$) can be determined with the molar mass. Similar to the calculations in chapter 4.2.2 Equation 6 is used. The calculated mass concentration (g/L) is then transformed into a mass flow (kg/d) multiplying with the volumetric flow (L/d) and Equation 7.

5. RESULTS AND DISCUSSION

5.1. RATE OF ACID PRODUCED PER DAY

Using Equation 5 and the data shown in Appendix 1 the acid production rate for biotic pyrite oxidation was calculated to be 24.38 mol/day.

5.2. CHANGE IN H^+ CONCENTRATION OVER TIME

The initial H^+ concentration of 0.0021 mol/L was given with the pH and then the calculated concentration of produced acid by the *A.ferroxidans* was added to the excel sheet (see Appendix 2). Figure 4 shows the increase in the H^+ concentration over time.

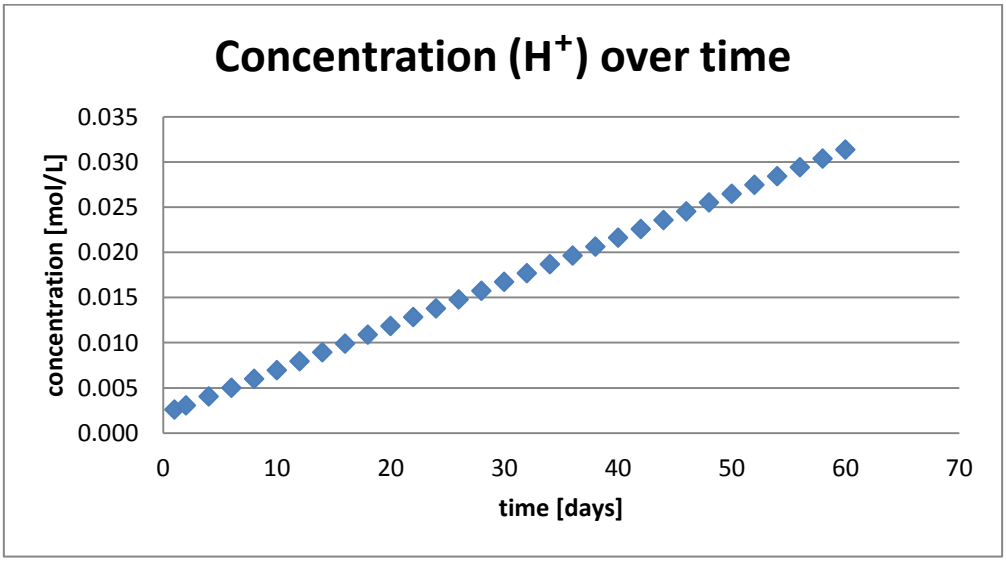

Figure 4 showing the initial H^+ concentration (0.0021 mol/L) increases over time with the added acid produced by A. ferrooxidans

5.3. MASS FLOW OF SULPHURIC ACID

The initial mass flow of sulphuric acid (H_2SO_4) was calculated to be 12.64 kg/d. However this mass flow was increasing vastly over time due to the process of pyrite oxidation. After 46 days the mass flow was multiplied by 10 compared to the initial mass flow. Figure 5 shows the trend of the mass flow-curve over time.

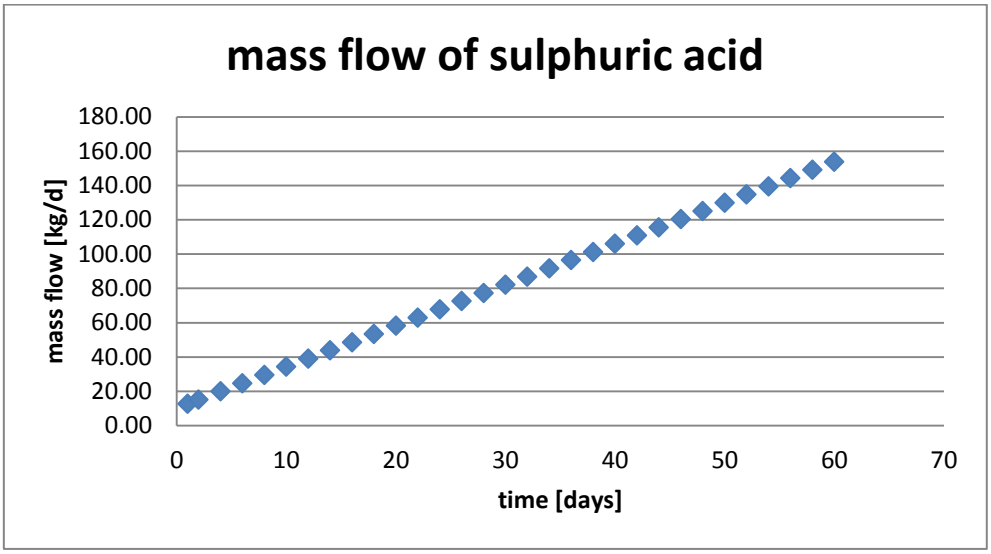

Figure 5. The sulphuric acid mass flow [kg/d] over time

5.4. pH - CHANGE OVER TIME

With Equation 6 the trend of pH over time can be calculated and the decrease in the pH is illustrated in Figure 6. The pH decreases from the initial pH of 2.68 to a pH of 2 within 16 days and after 60 days it reaches the pH of 1.5. These results seem realistic as it is known that *A.ferrooxidans* can decrease the pH to less than pH 1 over a few days.

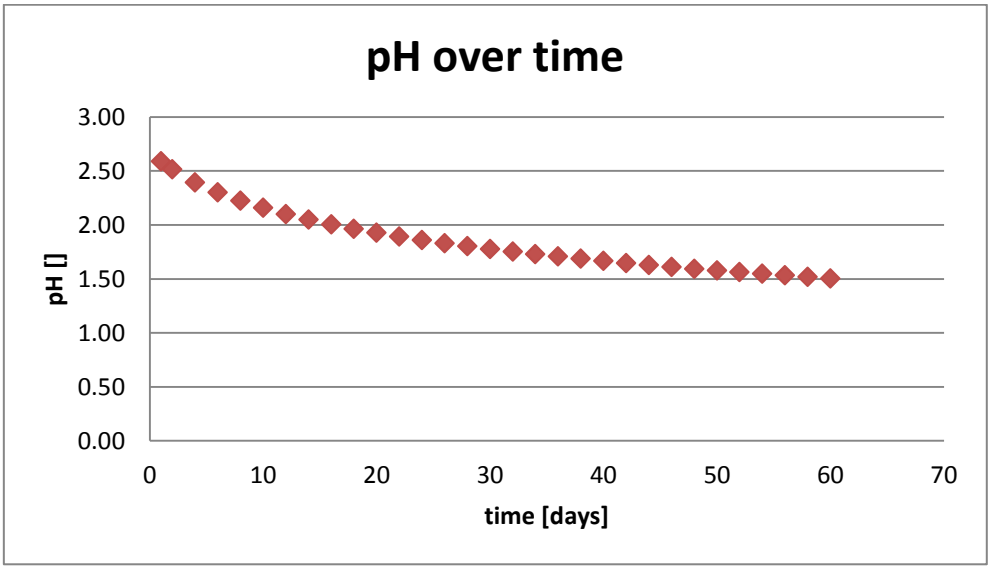

Figure 6. pH change over time

Comparing the results to earlier laboratory results from a media optimisation trial for *A.ferrooxidans* (Appendix 3), the calculated pH coincides reasonably. Although the laboratory data shows an increase in pH on the first day, which is related to the growth phases of the bacterium, the pH decreases within 10 days from the initial pH of 4 to a pH of ~2, depending on the media.

This implies that the calculated data is reasonable and the box model can be used for further analysis. However, the missing input data has to be adjusted to the specific site.

5.5. MASS FLOW OF CALCIUM CARBONATE

As the same mole concentration of calcium carbonate is required to neutralise the acidic conditions with a certain concentration of sulphuric acid, the daily required amount of calcium carbonate is equally increasing with the produced acid concentration, shown in Figure 4. Figure 7 displays the mass flow of calcium carbonate ($CaCO_3$) over time, which is required to neutralise the decreasing pH, shown in Figure 7. Hereby it should be considered, that the amount of calcite is only a minimum value and it should be added in excess.

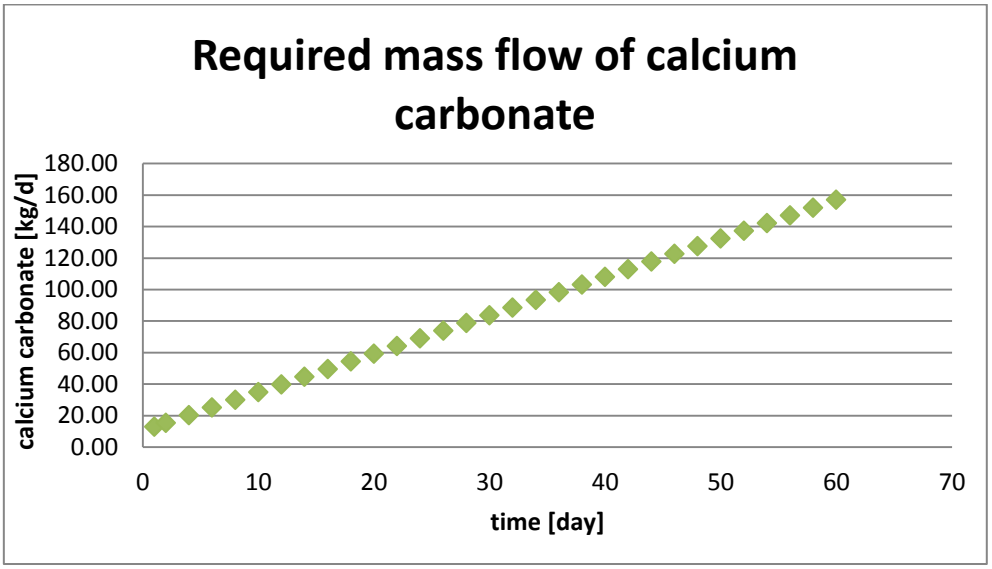

Figure 7 displaying the increase in required mass flow of calcium carbonate over time

5.6. The Influence of Pyrite oxidation on Heavy Metals and Uranium

As discussed earlier, a decrease in pH can have a significant influence on the mobilisation of heavy metals and uranium. The researchers working with the Western Pits are especially concerned about the uranium and the radio activity of the acid mine drainage effluents.

Looking at case studies conducted by Merkel et al. (2008), ion concentrations were measured in the absence and presence of calcite and the overall result showed that calcite definitely has an impact of the acidity of the system. When pyrite weathering takes place in absence of calcite the pH falls from 6.3 to 0.7 and when calcite is present the pH only decreases from 6.9 to 5.1, this implies a buffer effect as explained in chapter 4.3.

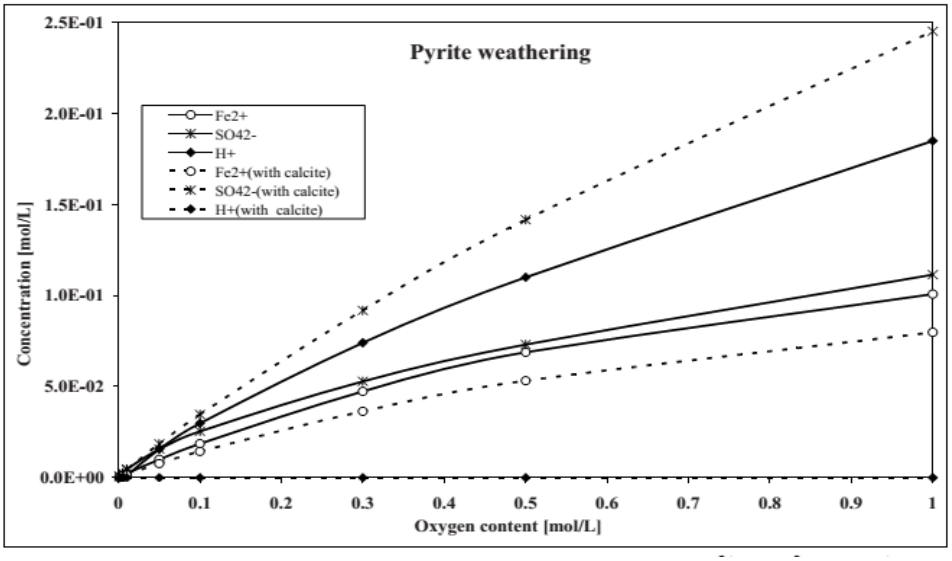

Figure 8. Influence of pyrite oxidation on iron(II), sulphate and H+ concentrations in the absence and presence of calcite (Merkel et al., 2008)

As shown in Figure 8, the ion concentrations of sulphate (SO_4^{2-}), iron (Fe^{2+}) and H^+ were measured in presence and absence of calcite. Iron and H^+ significantly decreased in the presence of calcite as bicarbonate (HCO_3^-) and iron-bicarbonate ($FeHCO_3^+$) complexes are formed. On the other side the sulphate (SO_4^{2-}) increased due to the formation of bicarbonate that consumed all the H^+ ions and no H^+ was left to form bisulphate (HSO_4^-). However it is important to see that metals such as iron are bound in complexes and are not mobile when calcite is present.

When the mineral phase U_3O_8 is present, the mobilised uranium concentration is higher when no calcite is present in the solution. In the presence of calcite the concentration of uranium is only 1/100,000 of the amount that was soluble when no calcite was present (Merkel et al., 2008). Hence, the presence of calcite supports the immobilisation of uranium significantly.

6. CONCLUSION AND RECOMMENDATIONS

Considering the weak data basis for the excel sheet input and that the majority of input values was assumed, the final results of box model were reasonable when compared to literature results and general knowledge. The results of the evolved excel sheet cannot be considered completely realistic, but they give a first impression of the intensity of possible bio-geochemical reactions and at which rate acid is produced.

To elaborate the box model further, the missing input data have to be developed with laboratory work and experimental field data. The specificity of the data available for this report was very limited and therefore the majority of the results are not site specific. However this shortcoming can be improved easily with work being conducted at the site to obtain the needed data.

Consequently biotic pyrite oxidation reduces the pH significantly and mobilises heavy metals and uranium. It was suggested to prevent this mobilisation and the pH decrease with the addition of calcite at the outflow point. Another idea would be to add calcite into the mine shafts or directly to the mine dumps as well. Thus the water would reach to the mine shaft less acidic and pyrite oxidation would only take place at a lesser extent.

7. REFERENCES

Bell, F.G., 1998. Environmental geology principles and practice. Blackwell Science, Oxford; Malden, Mass.

Bishop, M., 2002. An introduction to chemistry. Benjamin Cummings, San Francisco.

Casas, I., de Pablo, J., Giménez, J., Torrero, M.E., Bruno, J., Cera, E., Finch, R.J., Ewing, R.C., 1998. The role of pe, pH, and carbonate on the solubility of UO2 and uraninite under nominally reducing conditions. Geochim. Cosmochim. Acta 62, 2223–2231. doi:10.1016/S0016-7037(98)00140-9

City of Johannesburg, 2014. city of Johannesburg - Mining [WWW Document]. URL http://www.joburg.org.za/index.php?option=com_content&view=article&id=103:mining&catid=30&Itemid=58 (accessed 3.8.14).

Colmer, A.R., Hinkle, M.E., others, 1947. The role of microorganisms in acid mine drainage: a preliminary report. Science 106, 253–256.

Gleisner, M., Herbert Jr., R.B., Frogner Kockum, P.C., 2006. Pyrite oxidation by Acidithiobacillus ferrooxidans at various concentrations of dissolved oxygen. Chem. Geol. 225, 16–29. doi:10.1016/j.chemgeo.2005.07.020

Greenpeace, 2011. Acid Mine Drainage in Johannesburg [WWW Document]. Greenpeace Afr. URL http://www.greenpeace.org/africa/en/News/news/Acid-Mine-Drainage/ (accessed 3.8.14).

Hawkins, A.B., 2014. Engineering implications of the oxidation of pyrite: an overview, with particular reference to Ireland, in: Implications of Pyrite Oxidation for Engineering Works. Springer, pp. 1–98.

Johnson, D.B., Hallberg, K.B., 2005. Acid mine drainage remediation options: a review. Sci. Total Environ. 338, 3–14. doi:10.1016/j.scitotenv.2004.09.002

Krug, E.C., Frink, C.R., 1983. Acid rain on acid soil: A new perspective. Science(Washington) 217, 520–525.

Lapakko, K.A., Antonson, D.A., 2006. Pyrite oxidation rates from humidity cell testing of greenstone rock, in: Conference Proceedings of 7th ICARD March. pp. 26–30.

Leduc, L.G., Ferroni, G.D., 1994. The chemolithotrophic bacterium Thiobacillus ferrooxidans. FEMS Microbiol. Rev. 14, 103–119. doi:10.1111/j.1574-6976.1994.tb00082.x

Merkel, B., Planer-Friedrich, B., Nordstrom, D.K., 2008. Groundwater geochemistry a practical guide to modeling of natural and contaminated aquatic systems, 2nd ed. ed. Springer, Berlin.

Turton, A., 2013. Debunking Persistent Myths about AMD in the Quest for a Sustainable Solution.

York, G., 2010. Poisonous water rising from the ground threatens Johannesburg [WWW Document]. Globe Mail. URL http://www.theglobeandmail.com/news/world/poisonous-water-rising-from-the-ground-threatens-johannesburg/article1319437/ (accessed 3.8.14).

APPENDIX 1 –Data input

Description	value	Unit	source
Biotic pyrite oxidation rate R_{FeS2-S}	1.92E-11	mol* m^{-2} *s^{-1}	for DO = 13.2µM
Molar mass of H_2SO_4	98.079	g/mol	true value
Molar mass of $CaCO_3$	100.0869	g/mol	true value
pH (IL8)	2.68	-	true value
c (H^+)	0.0020893	mol/l	calculated
Total volumetric flow	50000	L/day	example
DO (total) in µM	0.2037	µM	calculated
DO (total) in mg/l	6.52	mg/l	true value
Specific Surface area	0.147	m^2/g	example literature
mass of pyrite grains	50000000	g	example
stoichiometric factor for Eq	2	-	

APPENDIX 2 – Data output

time	n [mol]	conc [mol/l]	total c (H^+)	Mass flow (H2SO4)	pH	$CaCO_3$ [g/l]	$CaCO_3$ [kg/d]
1	24.39	0.0004877	0.002577	12.64	2.59	0.26	12.90
2	48.77	0.0009754	0.003065	15.03	2.51	0.31	15.34
4	97.54	0.0019508	0.004040	19.81	2.39	0.40	20.22
6	146.31	0.0029263	0.005016	24.60	2.30	0.50	25.10
8	195.08	0.0039017	0.005991	29.38	2.22	0.60	29.98
10	243.86	0.0048771	0.006966	34.16	2.16	0.70	34.86
12	292.63	0.0058525	0.007942	38.95	2.10	0.79	39.74
14	341.40	0.0068280	0.008917	43.73	2.05	0.89	44.62
16	390.17	0.0078034	0.009893	48.51	2.00	0.99	49.51
18	438.94	0.0087788	0.010868	53.30	1.96	1.09	54.39
20	487.71	0.0097542	0.011844	58.08	1.93	1.19	59.27
22	536.48	0.0107296	0.012819	62.86	1.89	1.28	64.15
24	585.25	0.0117051	0.013794	67.65	1.86	1.38	69.03
26	634.02	0.0126805	0.014770	72.43	1.83	1.48	73.91
28	682.80	0.0136559	0.015745	77.21	1.80	1.58	78.79
30	731.57	0.0146313	0.016721	82.00	1.78	1.67	83.68
32	780.34	0.0156067	0.017696	86.78	1.75	1.77	88.56
34	829.11	0.0165822	0.018671	91.56	1.73	1.87	93.44
36	877.88	0.0175576	0.019647	96.35	1.71	1.97	98.32
38	926.65	0.0185330	0.020622	101.13	1.69	2.06	103.20
40	975.42	0.0195084	0.021598	105.91	1.67	2.16	108.08
42	1024.19	0.0204839	0.022573	110.70	1.65	2.26	112.96
44	1072.96	0.0214593	0.023549	115.48	1.63	2.36	117.85
46	1121.73	0.0224347	0.024524	120.26	1.61	2.45	122.73
48	1170.51	0.0234101	0.025499	125.05	1.59	2.55	127.61
50	1219.28	0.0243855	0.026475	129.83	1.58	2.65	132.49
52	1268.05	0.0253610	0.027450	134.61	1.56	2.75	137.37
54	1316.82	0.0263364	0.028426	139.40	1.55	2.85	142.25
56	1365.59	0.0273118	0.029401	144.18	1.53	2.94	147.13
58	1414.36	0.0282872	0.030377	148.96	1.52	3.04	152.01
60	1463.13	0.0292626	0.031352	153.75	1.50	3.14	156.90

APPENDIX 3 – Earlier laboratory results from Bachelor thesis, Lisa Wild in 2012

The graph shows the pH (y-axis) in a medium over time on the x-axis.

The medium contained different concentrations of $CaCl_2$, KH_2PO_4, $MgSO_4$ * 7 H_2O, Na_2CO_3, $Na_2S_3O_3$, $(NH_4)_2SO_4$ and sulphide (S) and was inoculated with *Acidithiobacillus ferrooxidans* and *thiooxidans*.